SUPPLEMENTAL DATA

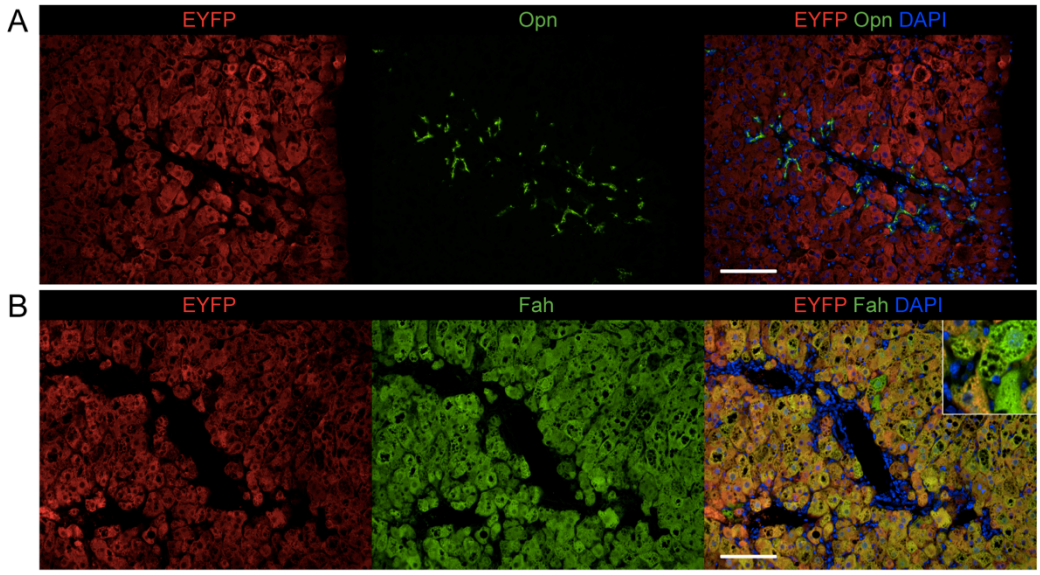

Figure S1. Additional Markers for Hepatocyte Fate Tracing in CDE Diet-Induced Chronic Liver Injury, Related to Figure 1

(A) Co-immunostaining for EYFP and Opn shows oval cell expansion characteristic for livers of mice after CDE diet feeding.

(B) Co-immunostaining for EYFP and Fah shows EYFP-negative, Fah-positive cells, i.e., non-fate-traced hepatocytes (inset).

Scale bars = 100 μm. Representative images from three mice are shown.

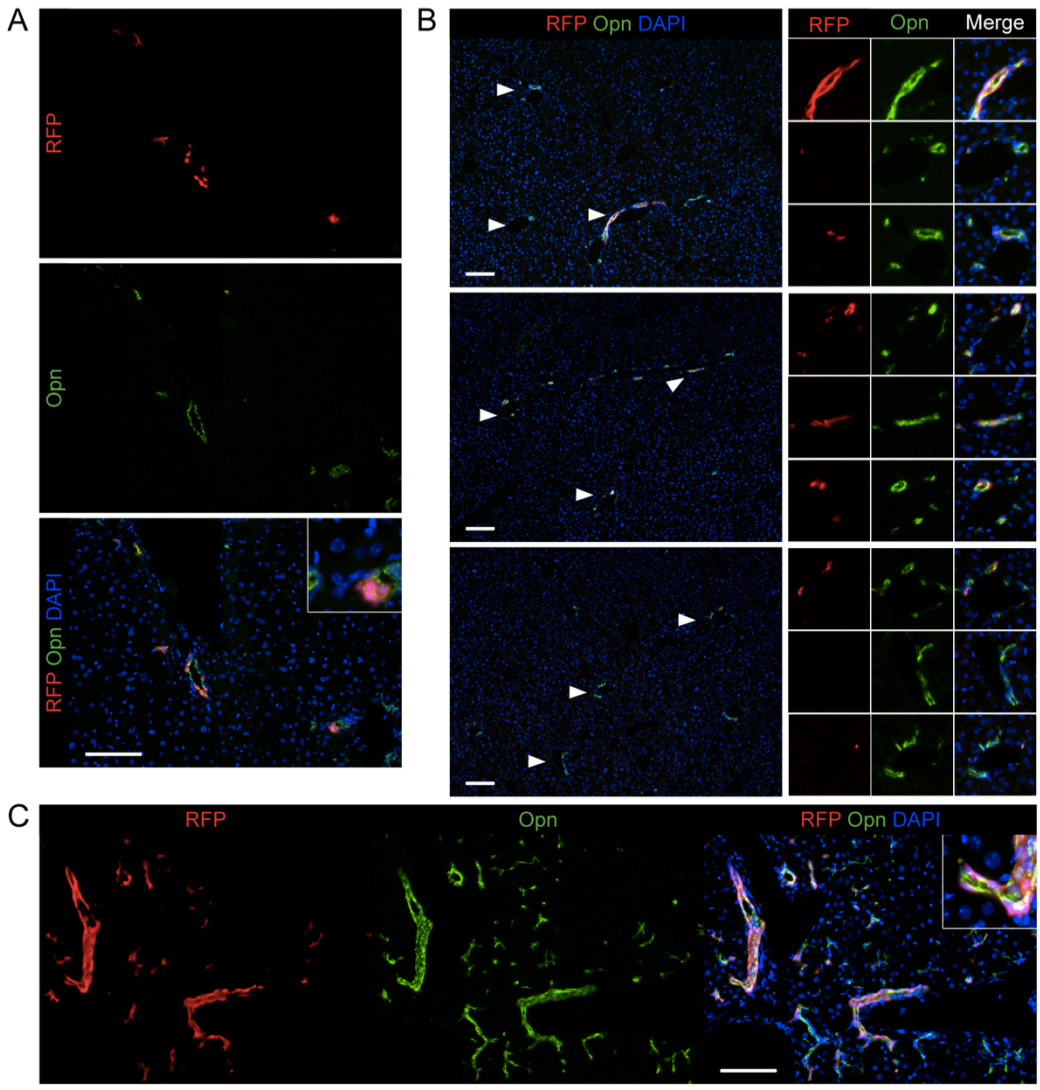

Figure S2. Specificity and Efficiency of Ck19-CreER Labeling in Non-Injured and Injured Livers, Related to Figure 2

(A) Ck19-CreER;R26R-RFP mice fed a normal diet were injected with 4 mg TAM every other day for four injections total. Livers were analyzed at least two weeks after the last injection. Direct fluorescence of RFP combined with immunostaining for Opn shows that BECs, but no other cell types, are RFP positive.

(B) Ck19-CreER;R26R-RFP mice fed a normal diet were injected with 4 mg TAM every other day for four injections total. Livers were analyzed two weeks after the last injection. Direct fluorescence of RFP combined with immunostaining for Opn shows intra-mouse variability in BEC labeling efficiency in three different mice (arrowheads).

(C) Periportal region of a Ck19-CreER;R26R-RFP mouse after TAM injection and CDE diet feeding. Direct fluorescence of RFP combined with immunostaining for Opn shows high BEC/oval cell labeling efficiency (> 50% of the Opn-positive cells are RFP positive), but no RFP-positive, Opn-negative cells, i.e., non-BECs/non-oval cells derived from BECs. Scale bars = 100 μm. Representative images from at least three mice are shown.

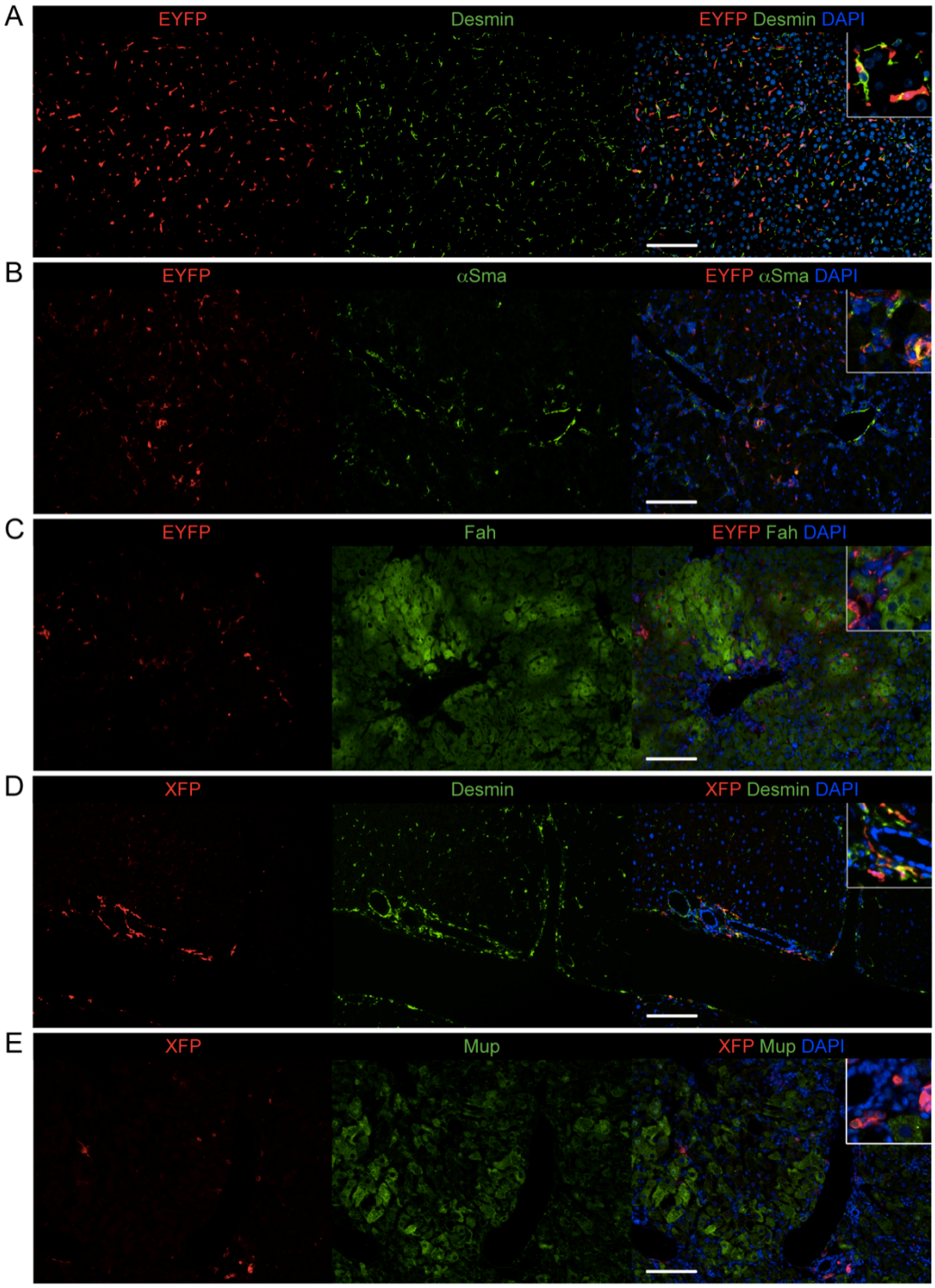

Figure S3. Specificity and Efficiency of Mesenchymal Cell Labeling in Non-Injured and Injured Livers, Related to Figure 3

(A) Co-immunostaining for EYFP and desmin shows that mesenchymal cells, but no other cell types, are EYFP positive in livers of Pdgfrb-Cre;R26R-EYFP mice fed a normal diet.

(B) Co-immunostaining for EYFP and αSma shows EYFP-positive, αSma-positive cells, i.e., fate-traced stellate cells/myofibroblasts, in livers of CDE diet-fed Pdgfrb-Cre;R26R-EYFP mice.
(C) Co-immunostaining for EYFP and Fah shows no EYFP-positive, Fah-positive cells, i.e., fate-traced hepatocytes, in livers of CDE diet-fed Pdgfrb-Cre;R26R-EYFP mice.
(D) Co-immunostaining for YFP/nGFP/mCFP (XFP) and desmin shows XFP-positive, desmin-positive periportal mesenchymal cells, but no XFP-positive cells with hepatocyte morphology, in livers of SM22-Cre;R26R-Confetti mice fed a normal diet.
(E) Co-immunostaining for YFP/nGFP/mCFP (XFP) and Mup or direct fluorescence for RFP (data not shown) shows no fate-traced hepatocytes—based on double-positive cells or morphology—in CDE diet-fed SM22-Cre;R26R-Confetti mice.
Scale bars = 100 μm. Representative images from at least three mice are shown.

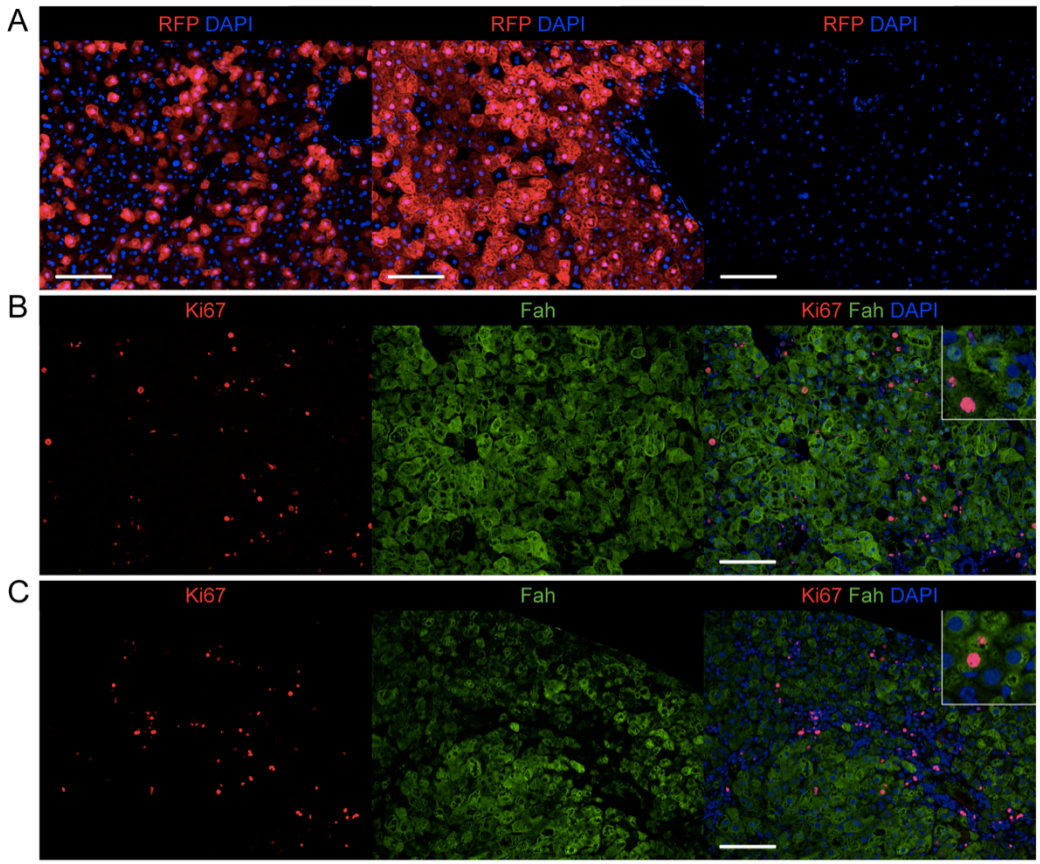

Figure S4. Additional Information About the Refined Hepatocyte Fate-Tracing Model and CDE Diet-Induced Chronic Liver Injury, Related to Figure 4

(A) Dose-dependent hepatocyte labeling in R26R-RFP mice by AAV8-Ttr-Cre. R26R-RFP mice were injected with AAV8-Ttr-Cre via the tail vein. The mouse shown in the left panel received half of the dose injected into the mouse shown in the middle panel. The R26R-RFP mouse shown in the right panel received no AAV8-Ttr-Cre. Livers were analyzed three days after injection. Direct fluorescence of RFP shows dose-dependent reporter activation after AAV8-Ttr-Cre injection and no reporter activation in the absence of AAV8-Ttr-Cre injection.

(B, C) Hepatocyte proliferation in livers of mice fed CDE diet. Co-immunostainings for the pan-proliferation marker Ki67 and Fah of livers of R26R-EYFP mice from Figure 1 (B) and livers of R26R-RFP mice from Figure 4 (C) show proliferating hepatocytes immediately after three weeks of CDE diet feeding. Representative images from three mice are shown.

Scale bars = 100 µm.

SUPPLEMENTAL EXPERIMENTAL PROCEDURES

Table S1. Primary Antibodies Used in This Study, Related to Figures 1-4

Antigen	Species	Dilution	Supplier
Ck19	Rabbit	1/100	Abbomax
Desmin	Rabbit	1/300	Thermo Scientific
Desmin	Goat	1/100	GenWayBio
GFP	Chicken	1/200	Abcam
Hnf4α	Mouse	1/100	Abcam
Ki67	Rabbit	1/100	Thermo Scientific
Ki67	Rat	1/100	Affymetrix
Mup	Goat	1/200	Cedarlane
Opn	Goat	1/250	R&D Systems
αSma	Rabbit	1/100	Abcam

Table S2. Secondary Antibodies Used in This Study, Related to Figures 1-4

Reactivity	Species	Fluorochrome	Dilution	Supplier
Chicken	Donkey	DyLight 549	1/200	Jackson Immunoresearch
Chicken	Donkey	Cy3	1/200	Jackson Immunoresearch
Goat	Donkey	Alexa Fluor 488	1/200	Molecular Probes
Goat	Donkey	DyLight 550	1/200	Pierce
Rabbit	Donkey	DyLight 488	1/200	Jackson Immunoresearch
Rabbit	Goat	DyLight 549	1/200	Jackson Immunoresearch
Rabbit	Donkey	DyLight 649	1/100	Millipore
Rat	Donkey	Alexa Fluor 647	1/200	Jackson Immunoresearch
Streptavidin		DyLight 488	1/100	Jackson Immunoresearch